

## ***Chop* deletion reduces oxidative stress, improves $\beta$ cell function, and promotes cell survival in multiple mouse models of diabetes**

Benbo Song, ... , Subramaniam Pennathur, Randal J. Kaufman

*J Clin Invest.* 2008;118(10):3378-3389. <https://doi.org/10.1172/JCI34587>.

Research Article

Metabolism

The progression from insulin resistance to type 2 diabetes is caused by the failure of pancreatic  $\beta$  cells to produce sufficient levels of insulin to meet the metabolic demand. Recent studies indicate that nutrient fluctuations and insulin resistance increase proinsulin synthesis in  $\beta$  cells beyond the capacity for folding of nascent polypeptides within the endoplasmic reticulum (ER) lumen, thereby disrupting ER homeostasis and triggering the unfolded protein response (UPR). Chronic ER stress promotes apoptosis, at least in part through the UPR-induced transcription factor C/EBP homologous protein (CHOP). We assessed the effect of *Chop* deletion in multiple mouse models of type 2 diabetes and found that *Chop*<sup>-/-</sup> mice had improved glycemic control and expanded  $\beta$  cell mass in all conditions analyzed. In both genetic and diet-induced models of insulin resistance, CHOP deficiency improved  $\beta$  cell ultrastructure and promoted cell survival. In addition, we found that isolated islets from *Chop*<sup>-/-</sup> mice displayed increased expression of UPR and oxidative stress response genes and reduced levels of oxidative damage. These findings suggest that CHOP is a fundamental factor that links protein misfolding in the ER to oxidative stress and apoptosis in  $\beta$  cells under conditions of increased insulin demand.

**Find the latest version:**

<https://jci.me/34587/pdf>





# *Chop* deletion reduces oxidative stress, improves $\beta$ cell function, and promotes cell survival in multiple mouse models of diabetes

Benbo Song,<sup>1</sup> Donalyn Scheuner,<sup>2</sup> David Ron,<sup>3</sup>  
Subramaniam Pennathur,<sup>4</sup> and Randal J. Kaufman<sup>1,2,4</sup>

<sup>1</sup>Howard Hughes Medical Institute and <sup>2</sup>Department of Biological Chemistry, University of Michigan Medical School, Ann Arbor, Michigan, USA.

<sup>3</sup>Skirball Institute of Biomolecular Medicine, New York University School of Medicine, New York, New York, USA.

<sup>4</sup>Department of Internal Medicine, University of Michigan Medical School, Ann Arbor, Michigan, USA.

**The progression from insulin resistance to type 2 diabetes is caused by the failure of pancreatic  $\beta$  cells to produce sufficient levels of insulin to meet the metabolic demand. Recent studies indicate that nutrient fluctuations and insulin resistance increase proinsulin synthesis in  $\beta$  cells beyond the capacity for folding of nascent polypeptides within the endoplasmic reticulum (ER) lumen, thereby disrupting ER homeostasis and triggering the unfolded protein response (UPR). Chronic ER stress promotes apoptosis, at least in part through the UPR-induced transcription factor C/EBP homologous protein (CHOP). We assessed the effect of *Chop* deletion in multiple mouse models of type 2 diabetes and found that *Chop*<sup>-/-</sup> mice had improved glycemic control and expanded  $\beta$  cell mass in all conditions analyzed. In both genetic and diet-induced models of insulin resistance, CHOP deficiency improved  $\beta$  cell ultrastructure and promoted cell survival. In addition, we found that isolated islets from *Chop*<sup>-/-</sup> mice displayed increased expression of UPR and oxidative stress response genes and reduced levels of oxidative damage. These findings suggest that CHOP is a fundamental factor that links protein misfolding in the ER to oxidative stress and apoptosis in  $\beta$  cells under conditions of increased insulin demand.**

## Introduction

Type 2 diabetes (T2D) is a world-wide disease of epidemic proportions that is estimated to afflict more than 180 million individuals, with approximately 2.9 million associated deaths per year (1, 2). Because loss of  $\beta$  cell function and mass are central events in the development and progression of T2D, they are key therapeutic targets for treatment of this disease (3, 4). In T2D,  $\beta$  cell toxicity has been linked to stimuli including glucose, lipids, proinflammatory cytokines, glycation products, and islet amyloid (4). Both signals from mitochondrial metabolism and oxidative stress are implicated in the  $\beta$  cell dysfunction of T2D (5–8). There is also a growing body of evidence to support the hypothesis that insulin resistance, a common underlying reason for the  $\beta$  cell failure that occurs in T2D, is associated with higher levels of ER stress in  $\beta$  cells in animal models of disease (9, 10) and also in humans (11, 12). It is proposed that increased proinsulin biosynthesis generates an unfolded/misfolded protein load in the ER lumen that activates the unfolded protein response (UPR) (9, 13). It is also hypothesized that misfolded islet amyloid precursor protein (IAPP) may accumulate in the ER lumen of  $\beta$  cells and cause apoptosis through induction of ER stress (11). Failure of the UPR to resolve misfolded protein and maintain ER homeostasis could lead to persistent ER stress and serve as a major determinant of  $\beta$  cell failure and death in diabetes.

A number of cellular insults disrupt protein folding and cause accumulation of unfolded protein in the ER lumen, including reduction in ER calcium stores, altered protein glycosylation, increased protein expression, unbalanced expression of protein subunits, or expression of difficult-to-fold or mutant inherently misfolded proteins. The UPR is an adaptive response signaled through 3 ER-localized transmembrane sensors, the protein kinases dsRNA-activated protein kinase-like ER kinase (PERK) and inositol-requiring protein 1 $\alpha$  (IRE1 $\alpha$ ) and the transcription factor activating transcription factor 6 (ATF6). This response collectively halts initiation of translation to reduce the load upon the ER; induces expression of protein chaperones, catalysts of folding, and protein degradation machinery; and also engages cellular death signaling (14, 15). PERK-mediated phosphorylation of the eukaryotic translation initiation factor 2 (eIF2) on Ser51 of the  $\alpha$  subunit (eIF2 $\alpha$ ) attenuates general mRNA translation. However, translation of some mRNAs is paradoxically increased, of which the mRNA encoding the transcription factor ATF4 is the most characterized example (16). IRE1 $\alpha$  is conserved in all eukaryotic cells and has protein kinase and endoribonuclease activities that, upon activation, mediate unconventional splicing of a 26-base intron from X-box binding protein 1 (*Xbp1*) mRNA to produce a potent transcription factor (17). ATF6 is a basic leucine zipper-containing transcription factor that, upon accumulation of unfolded protein in the ER lumen, transits to the Golgi compartment, where it is cleaved to yield a cytosolic fragment that migrates to the nucleus to activate gene transcription (18, 19). If the UPR adaptive response is not sufficient to resolve the protein-folding defect, ER dysfunction can aggravate cellular function and lead to apoptotic cell death (20, 21). Growing evidence supports the notion that UPR signaling improves ER homeostasis through attenuation of protein synthesis and increased ER-associated pro-

**Nonstandard abbreviations used:** ATF4, activating transcription factor 4; CHOP, C/EBP homologous protein; eIF2, eukaryotic translation initiation factor 2; GSIS, glucose-stimulated insulin secretion; HF, high fat; HOPE, hydroxyoctadecadienoic acid; IRE1 $\alpha$ , inositol-requiring protein 1 $\alpha$ ; PERK, dsRNA-activated protein kinase-like ER kinase; STZ, streptozotocin; T2D, type 2 diabetes; TEM, transmission electron microscopy; UPR, unfolded protein response; XBP1, X-box binding protein 1.

**Conflict of interest:** The authors have declared that no conflict of interest exists.

**Citation for this article:** *J. Clin. Invest.* 118:3378–3389 (2008). doi:10.1172/JCI34587.



tein degradation (ERAD). However, there is less compelling evidence that supports the idea that the UPR can improve the secretion capacity of the cell. The latter conclusion is largely inferred from gene deletion studies in which defects of ER stress signaling pathways reduce survival and/or differentiation of cells that secrete large amounts of protein.

It is now evident that conditions associated with high levels of ER stress can severely compromise  $\beta$  cell function (15). This is apparent from the  $\beta$  cell failure associated with mutations in murine and human proinsulin that disrupt disulfide bond pairing and cause misfolding and accumulation of proinsulin in the ER lumen of  $\beta$  cells (22–26). In addition, mutations that reduce signaling through the primary sensors of the UPR or interfere with protein chaperone functions of the UPR impair  $\beta$  cell health (9, 13, 27–31). Finally, stimuli, such as glucose, free fatty acids, cytokines, and nitric oxide compromise  $\beta$  cell function and induce UPR gene expression (12, 32–37). Fundamentally, glucose regulates both PERK-mediated eIF2 $\alpha$  phosphorylation and IRE1 $\alpha$ -mediated *Xbp1* mRNA splicing. Periodic increases in glucose, as well as chronic hyperglycemia, activate IRE1 $\alpha$  in vivo and in isolated rat islets (29, 38). Elevated glucose concentrations increase the rate of mRNA translation through phosphatase-mediated dephosphorylation of eIF2 $\alpha$ , and the unfolded protein load activates the UPR (38, 39). The significance of the PERK/eIF2 $\alpha$  pathway in supporting  $\beta$  cell function is underscored by the observation that mice and humans harboring loss-of-function mutations in PERK develop diabetes due to loss of  $\beta$  cell mass (13, 27, 40). In addition, homozygous missense *Ser51Ala* mutation at the PERK phosphorylation site in eIF2 $\alpha$  causes  $\beta$  cell deficiency in mice (28). Finally, heterozygous *Ser51Ala* eIF2 $\alpha$  mice fed a high-fat (HF) diet to induce insulin resistance develop  $\beta$  cell failure (9). These genetic alterations of both PERK and eIF2 $\alpha$  increase mRNA translation so that the protein-folding load exceeds the protein-folding capacity of the ER.

Although increasing evidence indicates that ER stress occurs in  $\beta$  cells, possibly as a consequence of increased proinsulin synthesis to compensate for insulin resistance, it is unknown whether  $\beta$  cell failure and loss of glucose homeostasis in vivo result from an inadequate UPR adaptive response or activation of an apoptotic response due to chronic, unresolved ER stress. As it is not possible to address this question in simple cell culture models of  $\beta$  cell apoptosis, we have studied whether the absence of CHOP, a key protein implicated in UPR-induced cell death, can prevent loss of  $\beta$  cell function and mass due to dietary or genetically induced insulin resistance in vivo.

CHOP was identified as an ER stress-induced transcription factor that is a significant mediator of apoptosis in response to ER stress (41, 42). *Chop* gene induction is primarily mediated through the PERK/eIF2 $\alpha$ /ATF4 UPR pathway, although IRE1 $\alpha$ /XBP1 and ATF6 $\alpha$  pathways also contribute (43–47). CHOP expression is increased in  $\beta$  cells from diabetic mice and humans (10–12, 48). Although *Chop*-null mice do not have a readily detectable phenotype under basal conditions (36, 41),  $\beta$  cells from *Chop*-null mice are protected from apoptosis caused by either nitric oxide (36) or accumulation of a folding-defective mutant of proinsulin (48). However, as CHOP is not the only death signal evoked by ER stress, the requirement for CHOP in  $\beta$  cell failure associated with T2D is unknown. Here, we show that *Chop* deletion increases the capacity of islets to produce insulin and curtails the progression of insulin resistance to diabetes. We demonstrate that deletion of *Chop* not only prevents  $\beta$  cell apoptosis, but also improves  $\beta$  cell function by preventing oxidative damage in

response to protein misfolding in the ER. The findings demonstrate that CHOP is a fundamental factor that links protein misfolding in the ER to oxidative stress and apoptosis in  $\beta$  cells.

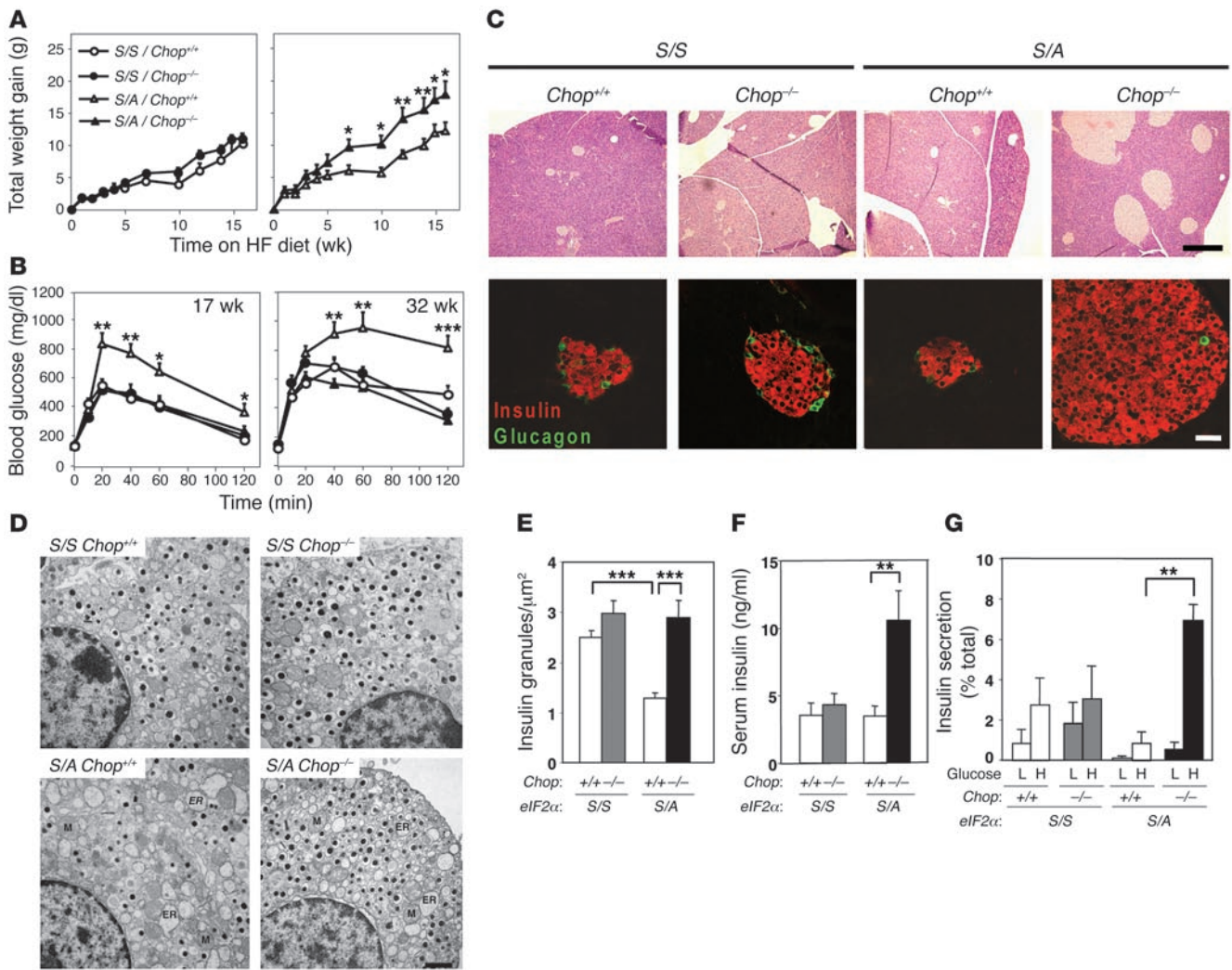
## Results

*Chop*-null mutation increases obesity but prevents glucose intolerance in HF diet-fed eIF2 $\alpha$ <sup>S/A</sup> mice. Although mice with heterozygous *Ser51Ala* mutation at the PERK phosphorylation site in eIF2 $\alpha$  exhibit reduced attenuation of mRNA translation upon ER stress, they did not exhibit a readily apparent phenotype under standard conditions of diet. Analysis of glucose-stimulated translation in islets isolated from HF diet-fed heterozygous *Ser51Ala* mice, however, revealed an elevated rate of translation (9). These HF diet-fed mice develop diabetes and represent what we believe to be a novel model of  $\beta$  cell failure that results from ER stress due to elevated proinsulin biosynthesis as a consequence of interaction between genetic (eIF2 $\alpha$ <sup>S/A</sup> allele) and environmental (HF diet) factors (9). We asked whether  $\beta$  cell survival and/or function are improved in these heterozygous *Ser51Ala* mutant mice when the CHOP-mediated death signal is absent. Deletion of the *Chop* gene modestly increased weight gain in HF diet-fed wild-type eIF2 $\alpha$ <sup>S/S</sup> mice, consistent with recent observations (49). In contrast, *Chop* deletion significantly increased obesity in HF diet-fed eIF2 $\alpha$ <sup>S/A</sup> mice (Figure 1A). The enhanced weight gain of eIF2 $\alpha$ <sup>S/A</sup>*Chop*<sup>-/-</sup> animals may be caused by accentuation of the metabolic defect previously reported for the eIF2 $\alpha$ <sup>S/A</sup> mice (9), may be a consequence of the deletion of CHOP action as a negative regulator of adipogenesis (50, 51), or may be driven by hyperinsulinemia (see below). Glucose intolerance appeared after 5 weeks of HF diet in eIF2 $\alpha$ <sup>S/A</sup>*Chop*<sup>+/+</sup> mice compared with HF diet-fed control eIF2 $\alpha$ <sup>S/S</sup>*Chop*<sup>+/+</sup> mice. In contrast, eIF2 $\alpha$ <sup>S/A</sup> mice with the *Chop*-null mutation displayed normal glucose tolerance for up to 32 weeks of HF diet despite their overt obesity (Figure 1B and Supplemental Figure 1A; supplemental material available online with this article; doi:10.1172/JCI34587DS1).

*Chop*-null mutation preserves  $\beta$  cell morphology and function in HF diet-fed eIF2 $\alpha$ <sup>S/A</sup> mice. The improved glucose tolerance observed in the eIF2 $\alpha$ <sup>S/A</sup>*Chop*<sup>-/-</sup> mice was not due to increased insulin sensitivity (Supplemental Figure 2A), but rather was associated with a 6-fold increase in islet mass and pancreas insulin content (Figure 1C and Supplemental Figure 1, B and C). Ultrastructural analysis was performed to monitor the distension of ER cisternae and reduction of secretory granule content characteristic of ER stress and  $\beta$  cell failure. Compared with  $\beta$  cells from HF diet-fed eIF2 $\alpha$ <sup>S/S</sup> mice,  $\beta$  cells from HF diet-fed eIF2 $\alpha$ <sup>S/A</sup>*Chop*<sup>+/+</sup> mice displayed a significantly distended ER and reduced insulin granule number, as previously reported (9). However, strikingly, the number of dense-core insulin granules in eIF2 $\alpha$ <sup>S/A</sup>*Chop*<sup>-/-</sup> mice was not significantly reduced compared with those in eIF2 $\alpha$ <sup>S/S</sup>*Chop*<sup>+/+</sup> mice or eIF2 $\alpha$ <sup>S/S</sup>*Chop*<sup>-/-</sup> mice, although ER distension was still detectable (Figure 1, D and E).

The improved glucose tolerance and preserved granule content suggested that *Chop* deletion preserves  $\beta$  cell function by maintaining an adequate pool of secretory granules that were responsive to nutrient stimuli. Consistent with this theory, after 35 weeks of HF diet, the serum insulin levels were increased 2- to 3-fold in eIF2 $\alpha$ <sup>S/A</sup>*Chop*<sup>-/-</sup> mice compared with eIF2 $\alpha$ <sup>S/S</sup>*Chop*<sup>+/+</sup>, eIF2 $\alpha$ <sup>S/S</sup>*Chop*<sup>-/-</sup>, and eIF2 $\alpha$ <sup>S/A</sup>*Chop*<sup>+/+</sup> mice (Figure 1F). Glucose-stimulated insulin secretion (GSIS) was significantly reduced in islets isolated from eIF2 $\alpha$ <sup>S/A</sup>*Chop*<sup>+/+</sup> mice compared with wild-type eIF2 $\alpha$ <sup>S/S</sup>*Chop*<sup>+/+</sup> mice



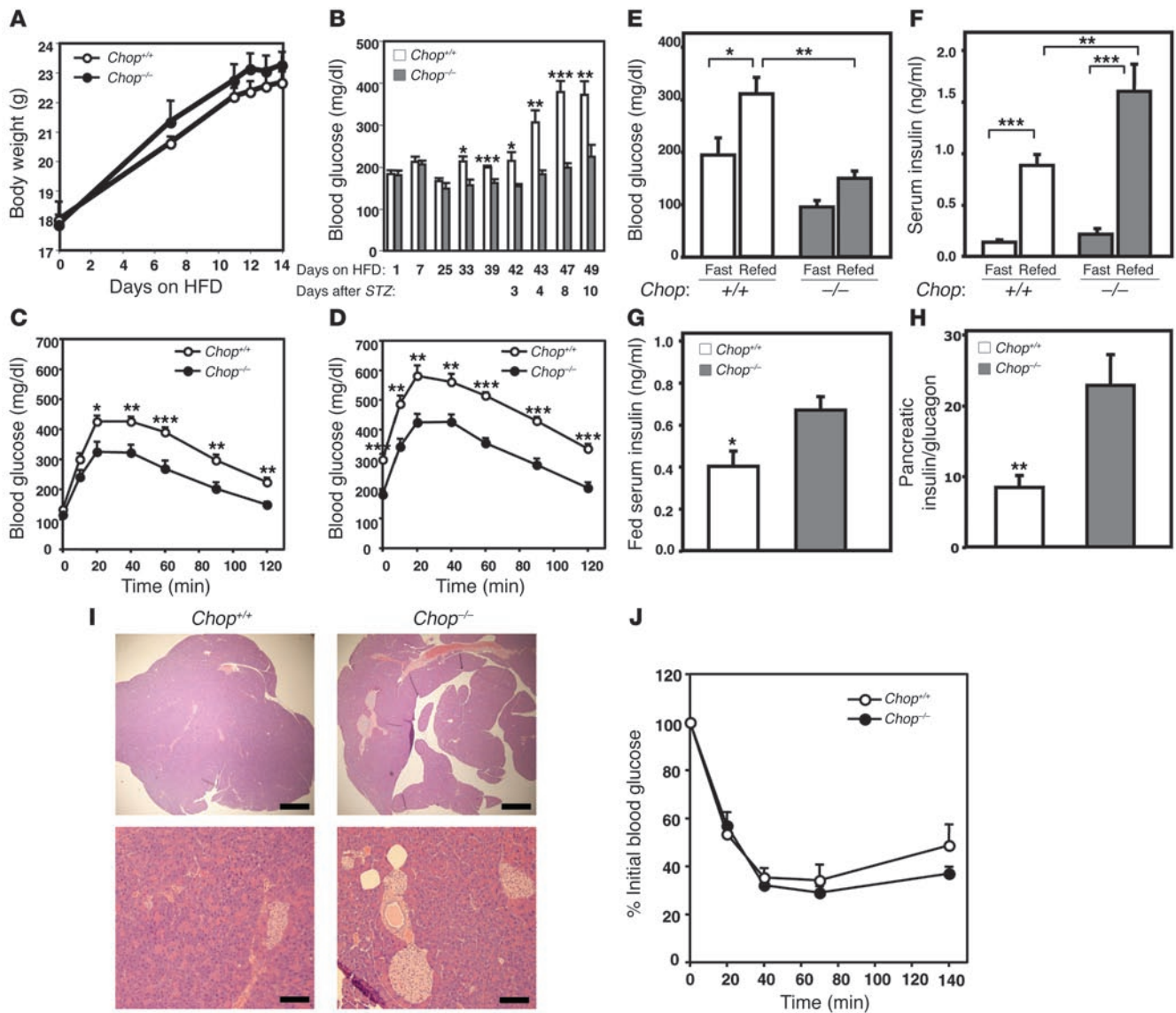


**Figure 1**

*Chop*-null mutation increases  $\beta$  cell mass, improves  $\beta$  cell function, and prevents glucose intolerance in HF diet-fed *eIF2 $\alpha$ <sup>S/A</sup>* mice. Mice of the indicated genotypes were fed a 45% HF diet for 35–41 weeks. (A and B) Body mass and glucose tolerance tests;  $n = 8$ –10 mice per condition. Significant differences between *eIF2 $\alpha$ <sup>S/A</sup>Chop<sup>+/+</sup>* and *eIF2 $\alpha$ <sup>S/A</sup>Chop<sup>-/-</sup>* are indicated. (C) Islet morphology shown by H&E and immunofluorescence staining. Scale bars: 400  $\mu$ m (top), 50  $\mu$ m (bottom). (D and E)  $\beta$  cell ultrastructure from TEM and insulin granule content quantified by analysis of similar total areas from TEM images from 2 mice per condition. ER, rough ER; M: mitochondria. Scale bar: 1  $\mu$ m. (F) Analysis of serum insulin levels;  $n = 8$ –10 mice per condition. (G) Analysis of GSIS. Islets from 2 animals per condition were analyzed in duplicate. H, high glucose (16.7 mM); L, low glucose (3.3 mM). \* $P < 0.05$ , \*\* $P < 0.01$ , \*\*\* $P < 0.001$ .

(Figure 1G). In contrast, islets from HF diet-fed *eIF2 $\alpha$ <sup>S/A</sup>Chop<sup>-/-</sup>* mice remained glucose responsive for insulin secretion (Figure 1G). As the GSIS studies were performed with selected islets of similar size and the secretion of insulin was expressed as a percentage of total insulin content, the improved GSIS observed in *eIF2 $\alpha$ <sup>S/A</sup>Chop<sup>-/-</sup>* islets was not due to increased  $\beta$  cell mass, but rather reflected a genuine improvement in  $\beta$  cell function. These findings show that, despite the HF diet and overt obesity, glucose homeostasis was maintained in *eIF2 $\alpha$ <sup>S/A</sup>Chop<sup>-/-</sup>* mice because there was an increase in the number of functional  $\beta$  cells as measured by insulin granule content and GSIS. The results suggest that  $\beta$  cell failure in this *eIF2 $\alpha$ <sup>S/A</sup>* mutant mouse model is mediated through the UPR-inducible gene *Chop*. This conclusion is also supported by the observation that *Chop* deletion reduced apoptosis and increased  $\beta$  cell mass in pancreata from homozygous *eIF2 $\alpha$ <sup>Ser51Ala</sup>* embryos (Supplemental Figure 3).

*Chop*-null mutation prevents loss of  $\beta$  cell mass and diabetes in a HF diet/streptozotocin model of T2D. The previous data indicated that CHOP plays a negative role in  $\beta$  cell function when ER stress signaling is compromised in conjunction with a biosynthetic burden of enhanced proinsulin translation due to insulin resistance. We next evaluated the role of CHOP under conditions that combine the primary determinants of T2D, insulin resistance, and inadequate  $\beta$  cell function and mass in the absence of a genetic predisposition to  $\beta$  cell failure. Wild-type and *Chop*-null mice were fed a 60% HF diet for 5–6 weeks, and  $\beta$  cell mass was reduced by administration of a moderate dose of streptozotocin (STZ). This treatment increases the proinsulin biosynthetic burden upon the remaining  $\beta$  cells and challenges their ability to survive and function. This approach has been successful in evaluating therapeutic strategies that alter insulin resistance or improve  $\beta$  cell function (52–54). In

**Figure 2**

*Chop*-null mutation prevents hyperglycemia and glucose intolerance by maintaining insulin content and secretion in a HF diet-fed, STZ-treated nongenetic model of T2D. *Chop*<sup>+/+</sup> and *Chop*<sup>-/-</sup> mice were fed a 60% HF diet (HFD) for 5.5 weeks prior to administration of a dosage of 150 mg/kg STZ as described in Methods, and measurements were performed for up to 16 days after STZ with continued HF feeding. (A) Body weight. (B) Fed blood glucose levels. (C and D) Glucose tolerance measurements. Glucose tolerance was tested after HF diet alone for 5.5 weeks (C) and 4 days after STZ treatment and continued HF diet (D). (E and F) Fasting and refed blood glucose and serum insulin levels. Glucose and insulin measurements were taken 13 days after STZ treatment from mice that were fasted overnight and refed for 3.5 hour. (G–I) Serum was collected for measurement and mice were sacrificed for determination of pancreatic insulin content and histology 16 days after STZ administration. (G) Fed serum insulin levels, (H) pancreatic insulin content, and (I) islet morphology stained with H&E. Scale bars: 500  $\mu$ m (top), 100  $\mu$ m (bottom). (J) Insulin tolerance measurements. Insulin tolerance was tested 15 days after STZ treatment. \* $P < 0.05$ , \*\* $P < 0.01$ , \*\*\* $P < 0.001$ .

the absence of any additional determinant of obesity, the *Chop*-null mice exhibited a slight increase in weight that was not statistically different from wild-type animals (Figure 2A). However, the fed glucose levels of *Chop*-null mice were significantly lower than those of wild-type mice after 5–6 weeks of HF diet feeding. In addition, the overt hyperglycemia that developed in wild-type mice 4 days after administration of STZ was averted in *Chop*-null mice (Figure 2B).

The improved glycemic control of *Chop*-null HF diet-fed, STZ-treated animals was investigated by analysis of glucose tolerance, insulin tolerance, insulin secretion, insulin content, and islet mor-

phology (Figure 2, C–J). In the absence of HF diet or with 45% HF feeding, glucose tolerance and  $\beta$  cell function were similar between wild-type and *Chop*<sup>-/-</sup> mice (Figure 1, Supplemental Figure 1, Figure 3, and Supplemental Figure 4). However, under conditions of 60% HF diet, glucose intolerance was more severe in wild-type mice compared with *Chop*<sup>-/-</sup> mice (Figure 2C). One week after STZ administration, the wild-type mice were severely hyperglycemic and glucose intolerant, while the *Chop*<sup>-/-</sup> mice were only mildly hyperglycemic and glucose intolerant (Figure 2, B and D). Blood glucose levels were 50% lower, and insulin secretion upon fasting and refeeding was signifi-



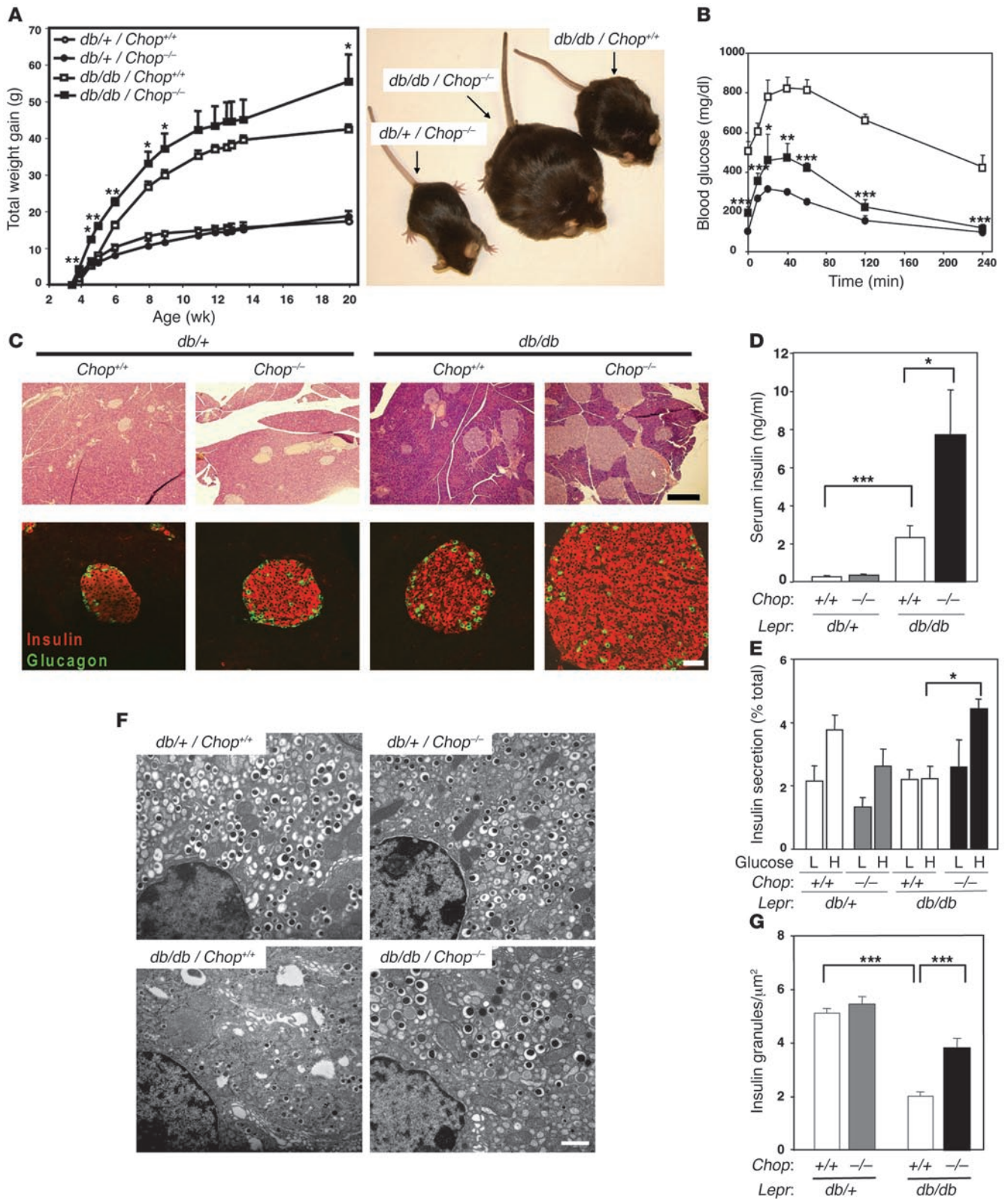


**Figure 3**

*Chop*-null mutation increases obesity and maintains glucose tolerance in *Lepr<sup>db/db</sup>* mice through expanded  $\beta$  cell mass and improved cell function. Analysis was performed on samples collected from mice at 9–10 (B–E) or 6 (F and G) months of age. (A) Body mass. Representative mice at 20 wk of age are shown. (B) Glucose tolerance tests;  $n = 3$ –5 mice per condition. Significant differences between *Lepr<sup>db/db</sup>Chop<sup>+/+</sup>* and *Lepr<sup>db/db</sup>Chop<sup>-/-</sup>* are indicated. (C) Islet morphology from H&E and immunofluorescence staining. Scale bars: 400  $\mu$ m (top), 50  $\mu$ m (bottom). (D) Serum insulin levels;  $n = 7$ –17 mice per condition. (E) GSIS analysis; islets from 2 mice per condition were analyzed in triplicate. (F and G) TEM images of  $\beta$  cells and insulin granule quantitation from similar total areas from 2 mice per condition. Scale bar: 1  $\mu$ m. \* $P < 0.05$ , \*\* $P < 0.01$ , \*\*\* $P < 0.001$ .

cantly elevated in *Chop*-null mice versus wild-type mice (Figure 2, E and F). Analysis of fed insulin levels, pancreatic insulin content, and islet morphology confirmed that the improved glucose homeostasis in the *Chop*-null mice was coincident with elevated basal insulin levels and a larger islet/ $\beta$  cell mass (Figure 2, G–I). There was no significant difference in insulin tolerance (Figure 2J). GSIS was not measured in islets isolated from these mice due to the low  $\beta$  cell mass of the wild-type mice in this model. However, in vitro STZ treatment of islets isolated from wild-type and *Chop*-null mice did not reveal any differences in the acute toxicity of STZ, as GSIS was fully inhibited in both populations of islets (data not shown), suggesting that *Chop* deletion influences subsequent  $\beta$  cell recovery and/or function.

*Chop*-null mutation prevents glucose intolerance and improves  $\beta$  cell function in *Lepr<sup>db/db</sup>* mice. We proceeded to investigate whether *Chop*-null mutation could prevent  $\beta$  cell loss in the leptin receptor-deficient *Lepr<sup>db/db</sup>* mouse, a model of diabetes that encompasses obesity, insulin resistance, and  $\beta$  cell failure. The  $\beta$  cell defects in the *Lepr<sup>db/db</sup>* mouse model depend on the C57BL/KsJ strain background. However, we were able to study the *Chop* contribution to  $\beta$  cell failure by analyzing first-generation littermates from crosses between double heterozygous *Chop<sup>+/-</sup>* and *Lepr<sup>db/+</sup>* mice in a mixed C57BL/KsJ and C57BL/6J background. All homozygous *Lepr<sup>db/db</sup>* progeny displayed hyperglycemia in the presence of the wild-type *Chop* allele, indicating there was sufficient C57BL/KsJ genetic contribution to elicit the diabetic phenotype.

Although the obesity of *Lepr<sup>db/db</sup>* mice was further increased by *Chop*-null mutation (Figure 3A), development of fasting hyperglycemia and glucose intolerance was dramatically prevented (Figure 3B and Supplemental Figure 4, A and B), similar to the effect of *Chop*-null mutation in the HF diet-fed *eIF2 $\alpha$ <sup>S/A</sup>* mice and HF diet-fed, STZ-treated mice. The improved glucose tolerance was not a consequence of increased sensitivity to insulin (Supplemental Figure 2B). Histological examination indicated that *Chop* deletion was associated with a 6-fold increase in islet mass in the *Lepr<sup>db/db</sup>* mice, and this correlated with serum hyperinsulinemia and glucose-responsive insulin secretion in vitro (Figure 3, C–E, and Supplemental Figure 4C). Ultrastructural analysis demonstrated that islets from *Lepr<sup>db/db</sup>* mice contained significantly fewer insulin granules than islets from *Lepr<sup>db/+</sup>* mice (Figure 3, F and G). In contrast, granule depletion was significantly attenuated in *Lepr<sup>db/db</sup>* mice that harbor *Chop* deletion (Figure 3, F and G). In summary, these studies suggest that *Chop* deletion improves  $\beta$  cell function in the *Lepr<sup>db/db</sup>* mouse.

*Chop*-null mutation causes  $\beta$  cell proliferation and reduces  $\beta$  cell apoptosis in the islets of *Lepr<sup>db/db</sup>* mice. To elucidate how *Chop* deletion may affect  $\beta$  cell mass, we studied  $\beta$  cell replication and apopto-

sis. TUNEL staining demonstrated that apoptosis was increased about 10-fold in the homozygous *Lepr<sup>db/db</sup>* mice compared with heterozygous *Lepr<sup>db/+</sup>* mice, similar to recent observations (55). However, *Chop* deletion dramatically reduced apoptosis in the *Lepr<sup>db/db</sup>* mice to levels observed in control *Lepr<sup>db/+</sup>* mice (Figure 4A). To evaluate  $\beta$  cell proliferation, BrdU-containing water was administered to mice prior to the development of full islet hyperplasia (56). As the rate of proliferation is very low in adult animals, a labeling period of 23 days was implemented to ensure accurate detection of altered proliferation rates. The number of BrdU-positive cells was approximately 2-fold greater in the islets from *Lepr<sup>db/db</sup>Chop<sup>-/-</sup>* mice compared with those from *Lepr<sup>db/db</sup>Chop<sup>+/+</sup>* mice (Figure 4B). Therefore, a portion of the islet hyperplasia observed in the *Chop*-null mice may be attributed to increased  $\beta$  cell proliferation, possibly a consequence of normal  $\beta$  cell compensation for insulin resistance. Therefore, the islet hyperplasia in *Lepr<sup>db/db</sup>Chop<sup>-/-</sup>* mice was a consequence of reduced apoptosis as well as increased proliferation.

*Chop*-null mutation increases expression of adaptive functions and reduces expression of apoptotic functions in *Lepr<sup>db/db</sup>* mice. To provide insight into how *Chop*-null mutation might alter the transcriptional profile to preserve  $\beta$  cell function, we analyzed isolated islets for expression of genes encoding functions in the UPR, the oxidative stress response, cell death, and insulin production (Figure 5). The expression of several UPR genes encoding adaptive functions to improve ER folding capacity, such as *BiP*, *Grp94*, *Fkbp11*, and *p58<sup>IPK</sup>*, was slightly increased in islets from *Lepr<sup>db/db</sup>Chop<sup>+/+</sup>* mice compared with control *Lepr<sup>db/+</sup>Chop<sup>+/+</sup>* mice. The expression levels of these genes were further increased in islets from *Lepr<sup>db/db</sup>Chop<sup>-/-</sup>* mice. In addition, there was increased splicing of *Xbp1* mRNA and expression of genes that encode components of the ER-associated protein degradation machinery, such as *Edem* and *Ubc7* (Figure 5A). The expression levels of several targets of CHOP that encode proapoptotic functions, i.e., *Gadd34*, *Dr5*, and *Trb3*, as well as other death pathway-related genes, were reduced in *Lepr<sup>db/db</sup>Chop<sup>-/-</sup>* islets (Figure 5C and Supplemental Figure 5A). The RT-PCR analyses also detected slightly increased expression of genes encoding functions that prevent oxidative stress, including *Sod1*, *Sod2*, *Gpx1*, *Pparg*, and *Ucp2*, in *Lepr<sup>db/db</sup>Chop<sup>+/+</sup>* islets. However, the expression of these genes was significantly elevated in *Lepr<sup>db/db</sup>Chop<sup>-/-</sup>* islets (Figure 5D). In contrast, expression of CHOP-dependent ER oxidoreductase 1 (*Ero1a*) (42), which generates oxidizing equivalents in the ER (16, 57), was decreased upon *Chop* deletion. Quantitative analysis of mRNA expression of other genes encoding ER stress proteins, transcription factors, other oxidative stress-related proteins, and  $\beta$  cell-specific genes did not clarify the mechanism by which *Lepr<sup>db/db</sup>Chop<sup>-/-</sup>*  $\beta$  cells adapt but may provide useful information for future studies (Supplemental Figure 5). As  $\beta$  cells express antioxidant functions at low levels (58, 59), these gene expression differences should minimize accumulation of ROS and facilitate adaptation. These findings support the hypothesis that *Chop* deletion improves  $\beta$  cell function as a consequence of increased expression of UPR adaptive and antioxidative stress response genes and reduced expression of proapoptotic functions.

*Chop*-null mutation reduces protein oxidation and lipid peroxidation in response to ER stress. The increased expression of genes encoding antioxidative stress responses suggested that *Chop* deletion improves the capacity of  $\beta$  cells to accommodate oxidative stress. Therefore, we measured products of protein oxidation (carbonyls) and lipid peroxidation (hydroxyoctadecadienoic acid [HODE]) in



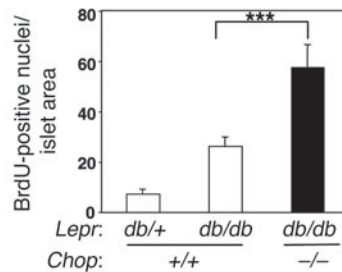
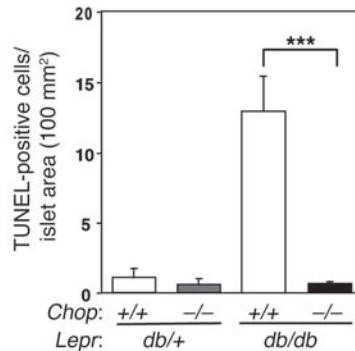
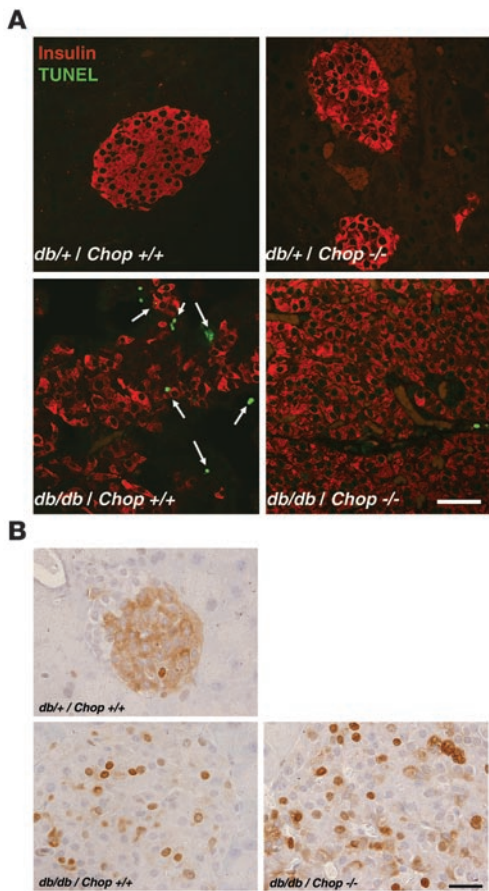


**Figure 4**

*Chop*-null mutation increases proliferation and reduces apoptosis within the islets of *Lepr<sup>db/db</sup>* mice. (A) Apoptosis. TUNEL staining was performed, and the number of positive cells (arrows) was quantified; *n* = 2–4 mice per condition. Scale bar: 50 μm. (B) Proliferation. BrdU-positive cells within islet areas were detected by immunohistochemistry, and the darkly stained nuclei were quantified from microscope images. Scale bar: 20 μm. \*\*\**P* < 0.001.

isolated islets. Islets from *Lepr<sup>db/db</sup>* diabetic mice displayed a 3-fold increase in protein carbonyls and a 2-fold increase in HODEs compared with those from control *Lepr<sup>db/+</sup>* mice (Figure 6A). Therefore, insulin resistance in the *Lepr<sup>db/db</sup>* mice was associated with oxidative stress in the islets, an observation consistent with literature that indicates antioxidant molecules can improve glucose homeostasis, restore β cell function, and reduce oxidative stress markers in the islets of *Lepr<sup>db/db</sup>* mice (55, 60–63). In contrast, *Chop* deletion significantly reduced both products of protein oxidation and lipid peroxidation in islets from these obese *Lepr<sup>db/db</sup>* mice.

The reduction in oxidative damage observed upon *Chop* deletion may be result from protection of the islets from oxidative damage caused by ROS or it may be an indirect consequence of improved glycemia (8, 64). To discriminate these possibilities, we analyzed islets in the absence of hyperglycemia and insulin resistance contributed by the *Lepr<sup>db/db</sup>* mutation. Islets were isolated from wild-type mice and *Chop<sup>-/-</sup>* mice and treated with tunicamycin to inhibit *N*-linked glycosylation and induce unfolded protein accumulation in vitro. Tunicamycin treatment increased protein oxidation and lipid peroxidation products 2.5- to 3-fold in wild-type islets (Figure 6B). In contrast, islets from *Chop<sup>-/-</sup>* mice displayed significantly reduced levels of carbonyls and HODEs after tunicamycin treatment. In addition, H<sub>2</sub>O<sub>2</sub> treatment increased levels of carbonyls and HODEs to similar extents in islets isolated from *Chop<sup>+/+</sup>* and *Chop<sup>-/-</sup>* mice (Figure 6C). Importantly, these results show that the *Chop*-null mutation protects β cells from oxidative damage that occurs in response to ER stress.

## Discussion

Studies in cultured cells indicate that acute UPR activation is an adaptive response to ER stress, whereas sustained UPR activation is associated with cell death (20). Recent studies have demonstrated that insulin resistance is associated with markers of UPR activation, including CHOP induction, in murine and human islets (10–12). However, it is not known whether UPR signaling is an adaptive mechanism that sustains β cell function and survival or whether UPR signaling contributes to β cell failure and death. To study this problem, we analyzed the role of the UPR in protein secretion and cell survival in vivo under conditions that pressure the β cell to produce elevated levels of insulin. Through deletion of the CHOP-mediated death signal, we have uncovered an important adaptive function of the UPR to limit oxidative stress in response to elevated protein secretion. Surprisingly, *Chop* deletion not only prevented UPR-induced death, but also improved the capacity of the β cell to produce insulin in 3 models of insulin resistance-induced β cell failure: heterozygous *Ser51Ala eIF2α* mutant mice fed a HF diet, mice fed a HF diet in conjunction with STZ treatment, and *Lepr<sup>db/db</sup>* mice as a genetic model of insulin resistance. In all models, *Chop* deletion preserved the β cell mass and improved β cell function, monitored by glucose homeostasis and GSIS. Finally, *Chop* deletion also attenuated the loss in β cell mass and apoptosis in embryonic homozygous *Ser51Ala eIF2α* mutant mice, a model of β cell demise that occurs in the absence of insulin resistance (Supplemental Figure 3). The sum of our findings support the idea that CHOP is a fundamental factor



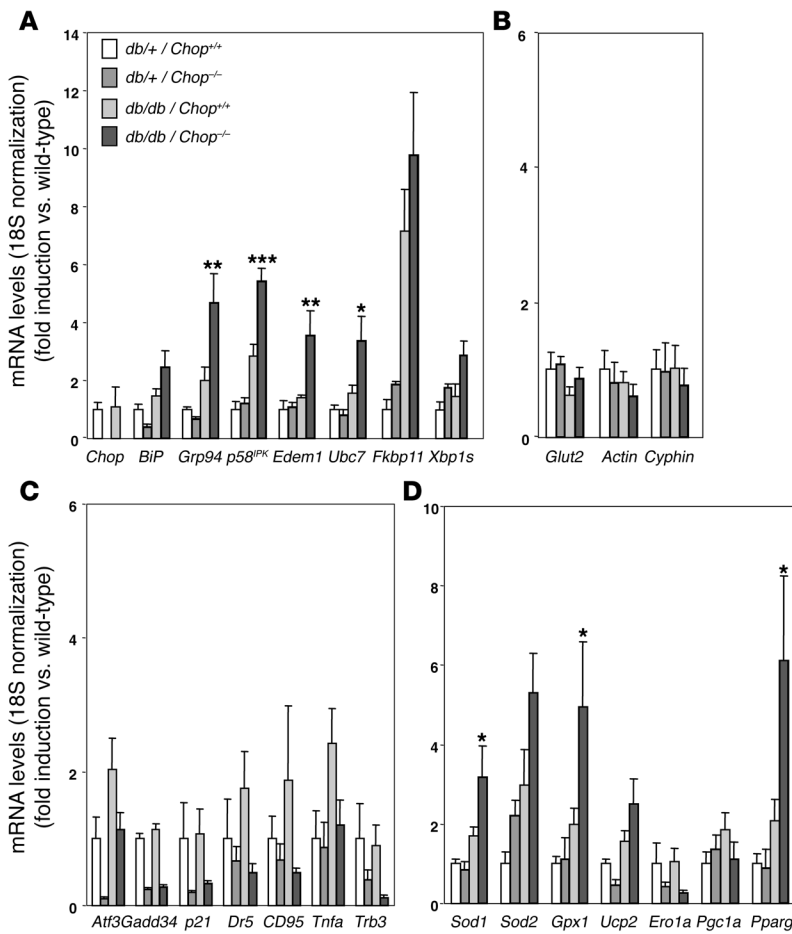


**Figure 5**  
*Chop*-null mutation in *Lepr<sup>db/db</sup>* mice increases expression of UPR and antioxidative stress response genes and decreases expression of proapoptotic genes. Real-time RT-PCR analysis of islet mRNA expression. Expression values were normalized to 18S rRNA and are presented as fold-induction compared with wild-type (*Lepr<sup>db/+</sup>Chop<sup>+/+</sup>*) islets. (A) UPR genes and ER-associated protein degradation genes. (B) Control genes. (C) CHOP-regulated genes and other death signaling genes. (D) Antioxidative stress genes. *Chop* mRNA was not detectable in *Lepr<sup>db/+</sup>Chop<sup>-/-</sup>* or *Lepr<sup>db/db</sup>Chop<sup>-/-</sup>* islets; *n* = 4–6 mice per condition. \**P* < 0.05, \*\**P* < 0.01, \*\*\**P* < 0.001 for *Lepr<sup>db/db</sup>Chop<sup>+/+</sup>* compared with *Lepr<sup>db/db</sup>Chop<sup>-/-</sup>*.

causing  $\beta$  cell failure and apoptosis in response to the chronic ER stress that coincides with  $\beta$  cell compensation for insulin resistance. Our findings indicate that in the absence of a death signal, UPR signaling can improve protein secretory capacity and preserve the functional integrity of the ER in  $\beta$  cells.

Our results support the hypothesis that *Chop* deletion improves ER function and protects against oxidative stress in response to ER stress in  $\beta$  cells. However, as our studies were performed in mice with *Chop* deletion in all tissues, the possibility exists that *Chop* deletion affects ER function in other tissues to alter organismal metabolism and, therefore,  $\beta$  cell function. Indeed, our findings as well as previously published results (49) demonstrate that *Chop* deletion can increase obesity. There are several possible mechanisms by which *Chop* deletion might increase obesity. First, *Chop* deletion might influence central nervous system regulation of appetite and/or metabolism. This is a topic that has not to our knowledge been explored. Second, since CHOP is highly expressed in the late stage of adipocyte differentiation and is a negative regulator of C/EBP $\alpha$  and C/EBP $\beta$  transcription factors, which are required for adipocyte differentiation (50), the absence of CHOP could increase signaling through the C/EBPs to increase both adipocyte differentiation and lipid biogenesis. As a consequence of the greater adiposity in *Chop*-null mice, more effective fatty acid storage could reduce  $\beta$  cell lipotoxicity. Since palmitate can cause ER stress in  $\beta$  cells (12, 32, 65, 66), improving sequestration of fatty acids could improve  $\beta$  cell function. Recent findings also indicate that ER stress can significantly affect lipid synthesis,

storage, and signaling (67, 68, 69). Therefore, the reduced ER stress as a consequence of *Chop* deletion could also reduce plasma lipids and lipid-induced  $\beta$  cell toxicity. Third, recent studies support the notion that ER stress may cause insulin resistance in liver and fat (70). Mice with reduced UPR signaling resulting from heterozygous deletion of *Xbp1* developed greater insulin resistance when fed a HF diet. In addition, treatment of leptin-deficient *ob/ob* mice with chemical chaperones, which are proposed to improve protein folding in the ER, reduced insulin resistance in fat and liver (71). If *Chop* deletion improves ER function, it may be expected to reduce insulin resistance and thereby improve  $\beta$  cell function by reducing pressure on the  $\beta$  cell to increase insulin production. However, we believe this is unlikely because insulin resistance was not apparently reduced in the *Chop*-null mice. Future studies should be directed to study the impact of *Chop* deletion on adipogenesis, insulin resistance, and lipid biosynthesis and storage. These studies and studies on appetite and metabolism would be most definitively performed in mice with conditional deletion of *Chop*. Although at present we cannot rule out potential effects of *Chop* deletion in other cell types, the protective effect of *Chop* deletion upon ER stress was observed in isolated islets (Figure 6B), indicating that the improved  $\beta$  cell function does not require other tissues.

Previous studies demonstrated that *Chop* deletion reduces apoptosis and delays glucose intolerance in heterozygous, but not homozygous, *Akita* mice that express *Cys96Tyr* misfolded proinsulin (48) and in  $\beta$  cells that are exposed to nitric oxide (36). However,

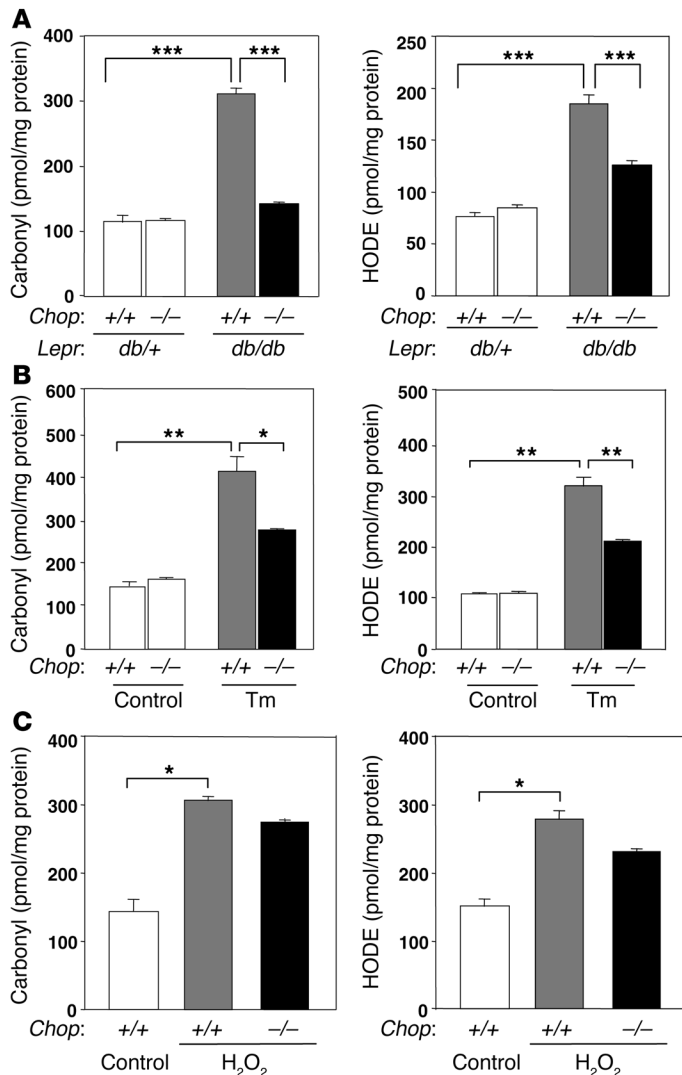


**Figure 6**  
*Chop*-null mutation protects from oxidative stress. (A–C) Oxidized proteins (carbonyls) and lipids (HODEs). (A) Direct analysis of islets isolated from mice of the indicated genotypes; *n* = 2–4 mice per condition. (B and C) Oxidation products measured in islets incubated in vitro. *Chop*<sup>+/+</sup> or *Chop*<sup>-/-</sup> islets were isolated, cultured overnight, and incubated with control media or media containing tunicamycin (2 μg/ml) for 10 hours (B) or 176 μM H<sub>2</sub>O<sub>2</sub> for 7 hours (C). \**P* < 0.05; \*\**P* < 0.01; \*\*\**P* < 0.001.

the molecular mechanism by which CHOP mediates β cell apoptosis under these conditions is not understood, and it is also not known whether protein misfolding in the ER contributes to death of β cells that produce wild-type proinsulin. Our findings demonstrate that *Chop* deletion prevents glucose intolerance by improving the β cell functional capacity of the ER to produce folded proinsulin and limit oxidative stress. This conclusion is supported by mRNA expression analysis that demonstrated *Chop* deletion was associated with increased expression of genes encoding antioxidative stress function, i.e., *Sod1*, *Sod2*, *Gpx1*, *Pparg*, and *Ucp2*.

Presently, most data support the idea that CHOP is induced by the PERK/eIF2α/ATF4 as well as the IRE1/XBP1 and ATF6 UPR subpathways to activate proapoptotic gene expression, restore trans-

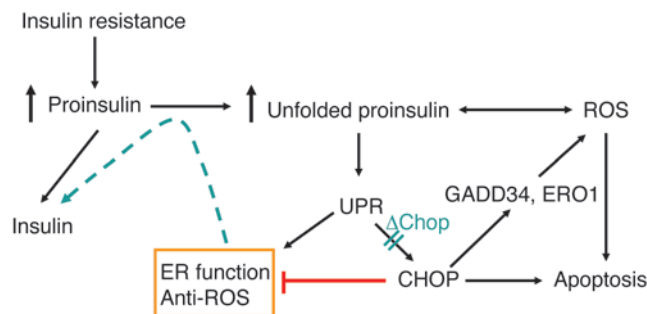
lation initiation, and increase the oxidizing potential in the ER lumen (42, 72). CHOP induces expression of GADD34, a subunit of type 1 protein phosphatase that directs eIF2α dephosphorylation to increase mRNA translation as homeostasis in the ER is restored (42, 73). CHOP is also implicated in the induction of ERO1α, a molecule that oxidizes protein disulfide isomerase (PDI) so it can function to rearrange improperly formed disulfide bonds within unfolded proteins. Disulfide bond formation during oxidative protein folding in the ER generates oxidative stress as a consequence of electron transfer from cysteine residues through PDI and ERO1 to molecular oxygen to form hydrogen peroxide (74, 75). Future studies should elucidate whether *Chop* deletion protects β cells from oxidative damage through the reduced expression of GADD34 and/or ERO1.

We have shown that increased protein misfolding in the ER increases oxidative damage in wild-type islets. Oxidative stress may further accentuate protein misfolding by directly modifying protein-folding intermediates, by disturbing protein chaperone functions, or by perturbing ER Ca<sup>2+</sup> homeostasis (76). Previous studies demonstrated that islets from *Lepr*<sup>db/db</sup> mice exhibit oxidative stress and neutralizing this stress can improve β cell function and prevent progression of T2D (62, 63). Indeed, antioxidant therapy has proven beneficial in diabetic animal models and possibly in humans with T2D (8, 60). Because they express low levels of antioxidant enzymes, β cells may be particularly sensitive to oxidative stress (58, 59). In addition, other stresses, such as proinflammatory cytokines, nitric oxide, hyperlipidemia, and hyperglycemia, may also produce ROS that could further disrupt protein folding in the ER lumen. We propose that oxidative damage that is caused by ER stress may be fundamental in the etiology of the β cell failure associated with both T1D and T2D.

Although the signaling pathways that are activated in response to misfolded protein accumulation in the ER have been identified, there is no evidence to support the idea that manipulation of these pathways can increase the protein folding and/or secretion potential of the ER. We believe our results, which show that deletion of the UPR-induced gene *Chop* improves the function of the secretory pathway, are the first example in which modulation of UPR signaling was demonstrated to preserve ER function. The improved ER function prevented β cell failure and the development of diabetes caused by insulin resistance and obesity. Although *Chop* was identified as an ER stress-induced transcription factor that mediates apoptosis, it is possible that changes in gene expression due to *Chop* deletion improve the functional capacity of the ER to reduce both protein misfolding and ER stress-mediated cell death signaling (Figure 7). Alternatively, in the absence of the CHOP-mediated death signal, UPR adaptive transcription may continue to improve the functional capacity of the ER. Further studies are required to elucidate how *Chop* deletion influences the transcriptional profile of the cell to preserve the functional capacity of the ER and reduce accumulation of ROS. Our findings should encourage the search for specific modulators of ER stress signaling that have the potential to improve the functional capacity of the ER for the treatment of numerous diseases associated with protein misfolding within this organelle.

**Methods**

**Animal husbandry.** *Ser51Ala eIF2α* mice (9) and *Chop*<sup>-/-</sup> mice (41) were backcrossed with C57BL/6J mice (The Jackson Laboratory). The *eIF2α*<sup>S/A</sup> and *Lepr*<sup>db/+</sup> mice (C57BKS.Cg-m<sup>+/+</sup> *Lepr*<sup>db</sup>, JAX mice) were bred with *Chop*<sup>-/-</sup>

**Figure 7**

Model depicting interrelationships between protein folding, UPR, CHOP, ROS, and apoptosis in  $\beta$  cells. The UPR induces genes to improve ER protein folding and reduce oxidative stress and also induces the proapoptotic gene *Chop*. CHOP enhances ROS formation, possibly through induction of GADD34 or ERO1. *Chop*-null mutation reduces proapoptotic gene expression to permit increased expression of UPR protective genes and antioxidative stress response genes to minimize ER stress and oxidative stress, thereby improving protein folding to support insulin production (depicted in blue). CHOP may also act, directly or indirectly, to repress transcription of some UPR protective genes or antioxidative stress response genes. Deletion of *Chop* in combination with insulin resistance increases  $\beta$  cell mass, reduces oxidative stress in islets, and preserves insulin secretion and glucose tolerance.

mice. All animals were housed at 21–23°C with 12-hour light/12-hour dark cycles in the Unit for Laboratory Animal Medicine at the University of Michigan Medical School, with free access to water and either standard rodent chow (LabDiet Formulab Diet, catalog 5008) or a 45% HF diet (Research Diets Inc.; catalog D12451) (Figure 1 and Supplemental Figures 1 and 2). Mice at 10–12 weeks of age were housed pair-wise and fed a HF diet for up to 41 weeks. All studies were performed with 8–10 male mice (except the study described in Supplemental Figure 4A, in which female mice were used) per experimental group. Body weights were measured weekly in the afternoon between 3 and 5 pm.

For all studies, age-matched littermates were utilized as controls. The effects of the *Chop*-null mutation were analyzed in *Lepr<sup>db/db</sup>* mice by comparison of littermates from crosses between *Lepr<sup>db/+</sup>Chop<sup>+/-</sup>* and *Lepr<sup>db/+</sup>Chop<sup>-/-</sup>* mice (Figures 3–5 and Supplemental Figures 2, 4, and 5). Additional groups of *Lepr<sup>db/+</sup>Chop<sup>+/+</sup>* and *Lepr<sup>db/+</sup>Chop<sup>-/-</sup>* mice were included in most studies to provide a comparison with non-diabetic control animals and for evaluation of any consequences of *Chop* deletion.

In the HF diet-fed, STZ-treated model of T2D, standard husbandry procedures were followed as described above, and 5- to 6-week-old *Chop<sup>+/-</sup>* and *Chop<sup>-/-</sup>* male mice were fed a 60% HF diet (catalog D12494; Research Diets Inc.) for 5–6 weeks prior to i.p. administration of 150 mg/kg STZ (Figure 2). All studies were performed with 7–13 mice per experimental group. Body weights and blood glucose levels were monitored in the morning between 9 and 11 am.

All procedures were conducted according to the protocols and guidelines approved by the University of Michigan Committee on the Use and Care of Animals (UCUCA).

**Glucose tolerance tests and blood glucose and serum insulin analysis.** Glucose tolerance was measured after i.p. injection of 2 g glucose/kg body weight (*eIF2 $\alpha$*  and HF diet-fed, STZ-treated mouse studies) or 1 g/kg (*Lepr<sup>db/db</sup>* mouse studies) to overnight-fasted animals. Blood glucose was measured using a OneTouch Ultra glucometer (LifeScan Inc.) with a sensitivity of 10 mg/dl. Serum insulin was measured with an ultrasensitive ELISA kit (Crystal Chem Inc.).

**Islet morphology and immunohistochemistry.** Pancreata were isolated, fixed with 10% buffered formalin, embedded in paraffin, sectioned, and stained with H&E for visualization by light microscopy. Insulin- and glucagon-containing cells were identified by immunofluorescence staining using guinea pig anti-human insulin antibody (Linco) with donkey anti-guinea pig Texas Red secondary antibody (Jackson ImmunoResearch) and rabbit anti-glucagon antibody (Linco) with goat anti-rabbit Alexa Fluor 488 secondary antibody (Invitrogen). Confocal images were recorded digitally by camera, and  $\beta$  cell mass was measured using Image-Pro Plus software (Media Cybernetics).

**Apoptosis assays and  $\beta$  cell proliferation.** BrdU incorporation was used to analyze  $\beta$  cell proliferation as previously described (56). To continuously label mice with BrdU for 23 days, we substituted drinking water containing 1 mg/ml BrdU dissolved in 0.007 N NaOH. BrdU water bottles were wrapped with aluminum foil to prevent light exposure, and freshly prepared solution was provided every other day. Pancreas tissue was harvested and processed as described above for immunohistochemistry. Sections were stained with BrdU In-Situ Detection Kit (BD Biosciences – Pharmingen), and replicating cells were counted from digital photographs obtained using a phase contrast microscope. The islet areas were quantified using Image-Pro Plus software (Media Cybernetics).

TUNEL assays were performed using the ApoAlert DNA Fragmentation Assay Kit (BD Biosciences – Clontech). Tissue sections from pancreata were first labeled for detection of insulin as described above, followed by TUNEL assay. Confocal images were recorded and TUNEL-positive cells were counted manually from the images. The islet areas for adult pancreatic sections were quantified using Image-Pro Plus software (Media Cybernetics).

**Pancreatic insulin content.** Pancreata were extracted by homogenization in a cold solution of acid/ethanol containing 80% ethanol and 0.19 M hydrochloric acid, sonicated on ice, and incubated at 4°C overnight (about 16–20 h). The extracts were then centrifuged, and supernatants were diluted into sample buffer. Insulin and glucagon contents were measured by ELISA (Crystal Chem Inc.) and radioimmunoassay (Glucagon RIA GL-32K; Linco Research Inc.), respectively.

**$\beta$  Cell ultrastructure.** Transmission electron microscopy (TEM) was performed on pancreas tissue (Figure 1D) and isolated islets (Figure 3F) as previously described (9). The number of insulin granules per islet area was determined using Image-Pro Plus software (Media Cybernetics).

**Islet isolation.** Islets of Langerhans were manually isolated after collagenase P (Roche) digestion and Ficoll gradient centrifugation (77, 78).

**GSIS.** Five islets of similar size were pre-incubated in basal glucose (3.3 mM) for 1 h at 37°C in Krebs-Ringer Bicarbonate HEPES buffer containing 129 mM NaCl, 5 mM NaHCO<sub>3</sub>, 4.8 mM KCl, 1.2 mM MgSO<sub>4</sub>, 1.2 mM KH<sub>2</sub>PO<sub>4</sub>, 1.0 mM CaCl<sub>2</sub>, and 10 mM HEPES at pH 7.4, plus 0.1% RIA-grade BSA (Sigma-Aldrich). Sequential static incubations were performed in low glucose (3.3 mM) for 15 or 30 min, followed by stimulatory incubation in high glucose (16.7 mM) for 30 min. Insulin release data are expressed as a percentage of total insulin content determined by a ratio of cold acid/ethanol lysis and ELISA.

**Gene expression analysis.** Total RNA was extracted from freshly isolated islets using RNeasy mini kit (Qiagen) for reverse-transcription into cDNA in a 20- $\mu$ l reaction using iScript cDNA Synthesis kit (BioRad). Reverse transcription reactions were incubated sequentially for 5 min at 25°C, 30 min at 42°C, and then 5 min at 85°C. cDNA products were stored at –20°C. iQ SYBR Green Supermix kit (Bio-Rad) was used for quantitative real-time PCR (20  $\mu$ l) using the iCycler iQ Real-Time PCR detection system (Bio-Rad). The thermal cycling parameters were as follows: step 1, 95°C for 10 min; step 2, 95°C for 15 s; step 3, 59°C for 1 min. Step 2 was repeated for 40 cycles. Reactions were terminated by incubation at 4°C. The relative amounts of mRNA were calculated from the Ct values using 18S rRNA for normalization. Primer sequences are presented in Supplemental Table 1.





**Quantitation of oxidation products.** Protein carbonyls were measured in islet extracts by ELISA (Biocell Corp.). Lipid peroxidation was quantified by detection of HODEs as previously described (79, 80). The islet protein content was determined by Bradford assay.

**Statistics.** Data are represented as mean ± SEM. Statistical significance of differences between groups was evaluated using the Student *t* test or 1-way ANOVA test (Tukey's test). *P* < 0.05 was considered statistically significant.

**Acknowledgments**

We gratefully thank Mary Pinter, Eric Liao, and Junying Wang for excellent technical assistance, Ming Liu and Peter Arvan for instruction in islet isolation technique, and Tom Rutkowski, Sung-Hoon Back, and David Ginsburg for critical review of the manuscript. We thank Janet Mitchell for her assistance in preparation of the manuscript and graphics. Electron, confocal, and light microscopy were performed at the University of Michigan Microscope and Image Analysis Lab (MIL). We thank Chris Edwards, Bruce Donohoe, Dotty Sorenson, Shelley Almburg, and Sasha Meshinchi of the MIL for their expertise and

assistance in these studies. This work was supported in part by NIH grants DK47119 and ES086811 (to D. Ron), DK42394, HL52173, and PO1 HL057346 (to R.J. Kaufman), and NIDDK 5P60DK020572 (to S. Pennathur) and Juvenile Diabetes Research Foundation Career Development Award 2-2003-149 (to S. Pennathur). R.J. Kaufman is an Investigator at the Howard Hughes Medical Institute.

Received for publication November 27, 2007, and accepted in revised form July 30, 2008.

Address correspondence to: Randal Kaufman, University of Michigan Medical Center, Departments of Biological Chemistry and Internal Medicine, H.H.M.I., 4570 MSRB II, 1150 W. Medical Center Dr., Ann Arbor, Michigan 48109-0650, USA. Phone: (734) 763-9037; Fax: (734) 763-9323; E-mail: kaufmanr@umich.edu.

Benbo Song and Donalyn Scheuner contributed equally to this work.

1. WHO. 2006. Diabetes [fact sheet]. <http://www.who.int/mediacentre/factsheets/fs312/en/>.
2. Roglic, G., et al. 2005. The burden of mortality attributable to diabetes: realistic estimates for the year 2000. *Diabetes Care*. **28**:2130–2135.
3. Wajchenberg, B.L. 2007. beta-cell failure in diabetes and preservation by clinical treatment. *Endocr. Rev.* **28**:187–218.
4. Prentki, M., and Nolan, C.J. 2006. Islet beta cell failure in type 2 diabetes. *J. Clin. Invest.* **116**:1802–1812.
5. Krauss, S., et al. 2003. Superoxide-mediated activation of uncoupling protein 2 causes pancreatic beta cell dysfunction. *J. Clin. Invest.* **112**:1831–1842.
6. Lowell, B.B., and Shulman, G.I. 2005. Mitochondrial dysfunction and type 2 diabetes. *Science*. **307**:384–387.
7. Brownlee, M. 2005. The pathobiology of diabetic complications: a unifying mechanism. *Diabetes*. **54**:1615–1625.
8. Robertson, R., Zhou, H., Zhang, T., and Harmon, J.S. 2007. Chronic oxidative stress as a mechanism for glucose toxicity of the beta cell in type 2 diabetes. *Cell Biochem. Biophys.* **48**:139–146.
9. Scheuner, D., et al. 2005. Control of mRNA translation preserves endoplasmic reticulum function in beta cells and maintains glucose homeostasis. *Nat. Med.* **11**:757–764.
10. Yusta, B., et al. 2006. GLP-1 receptor activation improves beta cell function and survival following induction of endoplasmic reticulum stress. *Cell Metab.* **4**:391–406.
11. Huang, C.J., et al. 2007. High expression rates of human islet amyloid polypeptide induce endoplasmic reticulum stress mediated beta-cell apoptosis, a characteristic of humans with type 2 but not type 1 diabetes. *Diabetes*. **56**:2016–2027.
12. Laybutt, D.R., et al. 2007. Endoplasmic reticulum stress contributes to beta cell apoptosis in type 2 diabetes. *Diabetologia*. **50**:752–763.
13. Harding, H.P., et al. 2001. Diabetes mellitus and exocrine pancreatic dysfunction in *per1-/-* mice reveals a role for translational control in secretory cell survival. *Mol. Cell*. **7**:1153–1163.
14. Ron, D., and Walter, P. 2007. Signal integration in the endoplasmic reticulum unfolded protein response. *Nat. Rev. Mol. Cell Biol.* **8**:519–529.
15. Scheuner, D., and Kaufman, R.J. 2008. The unfolded protein response: a pathway that links insulin demand with {beta}-cell failure and diabetes. *Endocr. Rev.* **29**:317–333.
16. Harding, H.P., et al. 2003. An integrated stress response regulates amino acid metabolism and resistance to oxidative stress. *Mol. Cell*. **11**:619–633.
17. Yoshida, H., Matsui, T., Yamamoto, A., Okada, T., and Mori, K. 2001. XBP1 mRNA is induced by ATF6 and spliced by IRE1 in response to ER stress to produce a highly active transcription factor. *Cell*. **107**:881–891.
18. Shen, J., Chen, X., Hendershot, L., and Prywes, R. 2002. ER stress regulation of ATF6 localization by dissociation of BiP/GRP78 binding and unmasking of Golgi localization signals. *Dev. Cell*. **3**:99–111.
19. Haze, K., Yoshida, H., Yanagi, H., Yura, T., and Mori, K. 1999. Mammalian transcription factor ATF6 is synthesized as a transmembrane protein and activated by proteolysis in response to endoplasmic reticulum stress. *Mol. Biol. Cell*. **10**:3787–3799.
20. Rutkowski, D.T., et al. 2006. Adaptation to ER stress is mediated by differential stabilities of pro-survival and pro-apoptotic mRNAs and proteins. *PLoS Biol.* **4**:e374.
21. Szegezdi, E., Logue, S.E., Gorman, A.M., and Samali, A. 2006. Mediators of endoplasmic reticulum stress-induced apoptosis. *EMBO Rep.* **7**:880–885.
22. Wang, J., et al. 1999. A mutation in the insulin 2 gene induces diabetes with severe pancreatic beta-cell dysfunction in the Mody mouse. *J. Clin. Invest.* **103**:27–37.
23. Herbach, N., et al. 2007. Dominant-negative effects of a novel mutated *Ins2* allele causes early-onset diabetes and severe {beta}-cell loss in Munich *Ins2C95S* mutant mice. *Diabetes*. **56**:1268–1276.
24. Stoy, J., et al. 2007. Insulin gene mutations as a cause of permanent neonatal diabetes. *Proc. Natl. Acad. Sci. U. S. A.* **104**:15040–15044.
25. Liu, M., Hodish, I., Rhodes, C.J., and Arvan, P. 2007. Proinsulin maturation, misfolding, and proteotoxicity. *Proc. Natl. Acad. Sci. U. S. A.* **104**:15841–15846.
26. Colombo, C., et al. 2008. Seven mutations in the human insulin gene linked to permanent neonatal/infancy-onset diabetes mellitus. *J. Clin. Invest.* **118**:2148–2156.
27. Delepine, M., et al. 2000. EIF2AK3, encoding translation initiation factor 2-alpha kinase 3, is mutated in patients with Wolcott-Rallison syndrome. *Nat. Genet.* **25**:406–409.
28. Scheuner, D., et al. 2001. Translational control is required for the unfolded protein response and in vivo glucose homeostasis. *Mol. Cell*. **7**:1165–1176.
29. Lipson, K.L., et al. 2006. Regulation of insulin biosynthesis in pancreatic beta cells by an endoplasmic reticulum-resident protein kinase IRE1. *Cell Metab.* **4**:245–254.
30. Ladiges, W.C., et al. 2005. Pancreatic beta-cell failure and diabetes in mice with a deletion mutation of the endoplasmic reticulum molecular chaperone gene P58IPK. *Diabetes*. **54**:1074–1081.
31. Oyadomari, S., et al. 2006. Cotranslocational degradation protects the stressed endoplasmic reticulum from protein overload. *Cell*. **126**:727–739.
32. Kharroubi, I., et al. 2004. Free fatty acids and cytokines induce pancreatic beta-cell apoptosis by different mechanisms: role of nuclear factor-kappaB and endoplasmic reticulum stress. *Endocrinology*. **145**:5087–5096.
33. Cardozo, A.K., et al. 2005. Cytokines downregulate the sarcoendoplasmic reticulum pump Ca2+ ATPase 2b and deplete endoplasmic reticulum Ca2+, leading to induction of endoplasmic reticulum stress in pancreatic beta-cells. *Diabetes*. **54**:452–461.
34. Pirot, P., Eizirik, D.L., and Cardozo, A.K. 2006. Interferon-gamma potentiates endoplasmic reticulum stress-induced death by reducing pancreatic beta cell defence mechanisms. *Diabetologia*. **49**:1229–1236.
35. Chambers, K.T., et al. 2007. The role of nitric oxide and the unfolded protein response in cytokine induced {beta}-cell death. *Diabetes*. **57**:124–132.
36. Oyadomari, S., et al. 2001. Nitric oxide-induced apoptosis in pancreatic beta cells is mediated by the endoplasmic reticulum stress pathway. *Proc. Natl. Acad. Sci. U. S. A.* **98**:10845–10850.
37. Lei, X., et al. 2007. The group VIA calcium-independent phospholipase A2 participates in ER stress-induced INS-1 insulinoma cell apoptosis by promoting ceramide generation via hydrolysis of sphingomyelin by neutral sphingomyelinase. *Biochemistry*. **46**:10170–10185.
38. Elouil, H., et al. 2007. Acute nutrient regulation of the unfolded protein response and integrated stress response in cultured rat pancreatic islets. *Diabetologia*. **50**:1442–1452.
39. Vander Mierde, D., et al. 2007. Glucose activates a protein phosphatase-1-mediated signaling pathway to enhance overall translation in pancreatic beta-cells. *Endocrinology*. **148**:609–617.
40. Zhang, W., et al. 2006. PERK EIF2AK3 control of pancreatic beta cell differentiation and proliferation is required for postnatal glucose homeostasis. *Cell Metab.* **4**:491–497.
41. Zinszner, H., et al. 1998. CHOP is implicated in programmed cell death in response to impaired function of the endoplasmic reticulum. *Genes Dev.* **12**:982–995.
42. Marciniak, S.J., et al. 2004. CHOP induces death by promoting protein synthesis and oxidation in the stressed endoplasmic reticulum. *Genes Dev.*



- 18:3066–3077.
43. Fawcett, T.W., Martindale, J.L., Guyton, K.Z., Hai, T., and Holbrook, N.J. 1999. Complexes containing activating transcription factor (ATF)/cAMP-responsive-element-binding protein (CREB) interact with the CCAAT/enhancer-binding protein (C/EBP)-ATF composite site to regulate Gadd153 expression during the stress response. *Biochem. J.* **339**:135–141.
44. Harding, H.P., et al. 2000. Regulated translation initiation controls stress-induced gene expression in mammalian cells. *Mol. Cell.* **6**:1099–1108.
45. Yamamoto, K., et al. 2007. Transcriptional induction of mammalian ER quality control proteins is mediated by single or combined action of ATF6alpha and XBP1. *Dev. Cell.* **13**:365–376.
46. Wu, J., et al. 2007. ATF6alpha optimizes long-term endoplasmic reticulum function to protect cells from chronic stress. *Dev. Cell.* **13**:351–364.
47. Acosta-Alvear, D., et al. 2007. XBP1 controls diverse cell type- and condition-specific transcriptional regulatory networks. *Mol. Cell.* **27**:53–66.
48. Oyadomari, S., et al. 2002. Targeted disruption of the Chop gene delays endoplasmic reticulum stress-mediated diabetes. *J. Clin. Invest.* **109**:525–532.
49. Ariyama, Y., et al. 2007. Chop-deficient mice showed increased adiposity but no glucose intolerance. *Obesity (Silver Spring)*. **15**:1647–1656.
50. Batchvarova, N., Wang, X.Z., and Ron, D. 1995. Inhibition of adipogenesis by the stress-induced protein CHOP (Gadd153). *EMBO J.* **14**:4654–4661.
51. Tang, Q.Q., and Lane, M.D. 2000. Role of C/EBP homologous protein (CHOP-10) in the programmed activation of CCAAT/enhancer-binding protein-beta during adipogenesis. *Proc. Natl. Acad. Sci. U. S. A.* **97**:12446–12450.
52. Luo, J., et al. 1998. Nongenetic mouse models of non-insulin-dependent diabetes mellitus. *Metabolism*. **47**:663–668.
53. Mu, J., et al. 2006. Chronic inhibition of dipeptidyl peptidase-4 with a sitagliptin analog preserves pancreatic beta-cell mass and function in a rodent model of type 2 diabetes. *Diabetes*. **55**:1695–1704.
54. Reed, M.J., et al. 2000. A new rat model of type 2 diabetes: the fat-fed, streptozotocin-treated rat. *Metabolism*. **49**:1390–1394.
55. Chu, K.Y., and Leung, P.S. 2007. Angiotensin II Type 1 receptor antagonism mediates uncoupling protein 2-driven oxidative stress and ameliorates pancreatic islet beta-cell function in young Type 2 diabetic mice. *Antioxid. Redox Signal.* **9**:869–878.
56. Teta, M., et al. 2005. Very slow turnover of beta-cells in aged adult mice. *Diabetes*. **54**:2557–2567.
57. Sevier, C.S., et al. 2007. Modulation of cellular disulfide-bond formation and the ER redox environment by feedback regulation of Ero1. *Cell*. **129**:333–344.
58. Lenzen, S., Drinkgern, J., and Tiedge, M. 1996. Low antioxidant enzyme gene expression in pancreatic islets compared with various other mouse tissues. *Free Radic. Biol. Med.* **20**:463–466.
59. Sigfrid, L.A., et al. 2004. Antioxidant enzyme activity and mRNA expression in the islets of Langerhans from the BB/S rat model of type 1 diabetes and an insulin-producing cell line. *J. Mol. Med.* **82**:325–335.
60. Kaneto, H., et al. 1999. Beneficial effects of antioxidants in diabetes: possible protection of pancreatic beta-cells against glucose toxicity. *Diabetes*. **48**:2398–2406.
61. Gorigawa, S., et al. 2002. Probucol preserves pancreatic beta-cell function through reduction of oxidative stress in type 2 diabetes. *Diabetes Res. Clin. Pract.* **57**:1–10.
62. Ishida, H., et al. 2004. Pioglitazone improves insulin secretory capacity and prevents the loss of beta-cell mass in obese diabetic db/db mice: Possible protection of beta cells from oxidative stress. *Metabolism*. **53**:488–494.
63. Yamamoto, M., et al. 2008. Transgenic expression of antioxidant protein thioredoxin in pancreatic beta cells prevents progression of type 2 diabetes mellitus. *Antioxid. Redox Signal.* **10**:43–49.
64. Kaneto, H., et al. 2007. Involvement of oxidative stress in the pathogenesis of diabetes. *Antioxid. Redox Signal.* **9**:355–366.
65. Cunha, D.A., et al. 2008. Initiation and execution of lipotoxic ER stress in pancreatic {beta}-cells. *J. Cell Sci.* **121**:2308–2318.
66. Akerfeldt, M.C., et al. 2008. Cytokine-induced {beta}-cell death is independent of endoplasmic reticulum stress signaling. *Diabetes*. Online publication ahead of print. doi:10.2337/db07-1802.
67. Ramanadham, S., et al. 2004. Apoptosis of insulin-secreting cells induced by endoplasmic reticulum stress is amplified by overexpression of group VIA calcium-independent phospholipase A2 (iPLA2 beta) and suppressed by inhibition of iPLA2 beta. *Biochemistry*. **43**:918–930.
68. Lee, A.H., Scapa, E.F., Cohen, D.E., and Glimcher, L.H. 2008. Regulation of hepatic lipogenesis by the transcription factor XBP1. *Science*. **320**:1492–1496.
69. Oyadomari, S., Harding, H.P., Zhang, Y., Oyadomari, M., and Ron, D. 2008. Dephosphorylation of translation initiation factor 2alpha enhances glucose tolerance and attenuates hepatosteatosis in mice. *Cell Metab.* **7**:520–532.
70. Ozcan, U., et al. 2004. Endoplasmic reticulum stress links obesity, insulin action, and type 2 diabetes. *Science*. **306**:457–461.
71. Ozcan, U., et al. 2006. Chemical chaperones reduce ER stress and restore glucose homeostasis in a mouse model of type 2 diabetes. *Science*. **313**:1137–1140.
72. Ma, Y., Brewer, J.W., Diehl, J.A., and Hendershot, L.M. 2002. Two distinct stress signaling pathways converge upon the CHOP promoter during the mammalian unfolded protein response. *J. Mol. Biol.* **318**:1351–1365.
73. Connor, J.H., Weiser, D.C., Li, S., Hallenbeck, J.M., and Shenolikar, S. 2001. Growth arrest and DNA damage-inducible protein GADD34 assembles a novel signaling complex containing protein phosphatase 1 and inhibitor 1. *Mol. Cell Biol.* **21**:6841–6850.
74. Haynes, C.M., Titus, E.A., and Cooper, A.A. 2004. Degradation of misfolded proteins prevents ER-derived oxidative stress and cell death. *Mol. Cell*. **15**:767–776.
75. Tu, B.P., and Weissman, J.S. 2004. Oxidative protein folding in eukaryotes: mechanisms and consequences. *J. Cell Biol.* **164**:341–346.
76. Malhotra, J.D., and Kaufman, R.J. 2007. Endoplasmic reticulum stress and oxidative stress: a vicious cycle or a double-edged sword? *Antioxid. Redox Signal.* **9**:2277–2294.
77. Lacy, P.E., and Kostianovsky, M. 1967. Method for the isolation of intact islets of Langerhans from the rat pancreas. *Diabetes*. **16**:35–39.
78. Scharp, D.W., Kemp, C.B., Knight, M.J., Ballinger, W.F., and Lacy, P.E. 1973. The use of ficoll in the preparation of viable islets of langerhans from the rat pancreas. *Transplantation*. **16**:686–689.
79. Savenkova, M.L., Mueller, D.M., and Heinecke, J.W. 1994. Tyrosyl radical generated by myeloperoxidase is a physiological catalyst for the initiation of lipid peroxidation in low density lipoprotein. *J. Biol. Chem.* **269**:20394–20400.
80. Byun, J., Mueller, D.M., Fabjan, J.S., and Heinecke, J.W. 1999. Nitrogen dioxide radical generated by the myeloperoxidase-hydrogen peroxide-nitrite system promotes lipid peroxidation of low density lipoprotein. *FEBS Lett.* **455**:243–246.